Journal of Power Sources 196 (2011) 5742–5745

Contents lists available at ScienceDirect

Journal of Power Sources

journal homepage: www.elsevier.com/locate/jpowsour

Short communication

Non-aqueous manganese acetylacetonate electrolyte for redox flow batteries

Alice E.S. Sleightholme[a], Aaron A. Shinkle[a], Qinghua Liu[a,b], Yongdan Li[b], Charles W. Monroe[a], Levi T. Thompson[a,c,*]

[a] Department of Chemical Engineering, University of Michigan, Ann Arbor 48109-2136, USA
[b] Tianjin Key Laboratory of Catalysis Science and Technology and State Key Laboratory for Chemical Engineering, School of Chemical Engineering, Tianjin University, Tianjin 300072, China
[c] Department of Mechanical Engineering, University of Michigan, Ann Arbor 48109-2316, USA

ARTICLE INFO

Article history:
Received 17 December 2010
Received in revised form 2 February 2011
Accepted 3 February 2011
Available online 12 February 2011

Keywords:
Manganese acetylacetonate
Single-metal redox flow battery
Non-aqueous electrolyte
Organic
Energy-storage

ABSTRACT

A single-metal redox flow battery employing manganese(III) acetylacetonate in tetraethylammonium tetrafluoroborate and acetonitrile has been investigated. Cyclic voltammetry was used to evaluate electrode kinetics and reaction thermodynamics. The Mn^{II}/Mn^{III} and Mn^{III}/Mn^{IV} redox couples appeared to be quasi-reversible. A cell potential of 1.1 V was measured for the one-electron disproportionation of the neutral Mn^{III} complex. The diffusion coefficient for manganese acetylacetonate in the supporting electrolyte solution was estimated to be in the range of $3–5 \times 10^{-6}$ cm^2 s^{-1} at room temperature. The charge–discharge characteristics of this system were evaluated in an H-type glass cell. Coulombic efficiencies increased with cycling suggesting an irreversible side reaction. Energy efficiencies for this unoptimized system were ~21%, likely due to the high cell-component overpotentials.

1. Introduction

Redox flow batteries (RFBs) are being developed for applications including storage of the large amounts of energy produced by intermittent sources such as wind turbines and solar cells. Most RFB systems are based on aqueous electrolyte chemistries. These include Zn–Br [1], Fe–Cr [2], Br-polysulfide [3], and all-vanadium [4,5] RFBs. Since the energy and power densities of a battery are determined by the cell potential, the use of aqueous electrolytes limits system performance because the cell potential must lie within the potential range where the solvent and supporting electrolyte are electrochemically stable. Under standard conditions, the voltage limit for aqueous electrolytes is 1.23 V and operating temperatures are limited to 0–100 °C.

Our research group has been investigating non-aqueous RFB systems based on low-cost active materials from the family of metal β-diketonate coordination complexes. Non-aqueous electrolytes offer the possibility of wider stable potential windows, wider operating temperature ranges, and higher energy and power densities than aqueous electrolytes [6–10]. We recently reported results for vanadium acetylacetonate ($V(acac)_3$) [9] and chromium acetylacetonate ($Cr(acac)_3$) [10]. The $V(acac)_3$ and $Cr(acac)_3$ systems were quasi-reversible with cell potentials of 2.2 and 3.4 V, respectively.

Here we describe a single-element non-aqueous redox system comprised of manganese acetylacetonate ($Mn(acac)_3$) active species and tetraethylammonium tetrafluoroborate ($TEABF_4$) supporting electrolyte in acetonitrile (CH_3CN). While manganese complexes have been studied for use in aqueous RFBs [11], they have not previously been used in single-metal, non-aqueous RFBs. Results for this system are compared to the previously reported acetylacetonate complexes in an effort to identify trends that could be used for the design of non-aqueous electrolytes for RFBs. Cyclic voltammetry (CV) was used to evaluate the cell potential and kinetic behavior. Charge–discharge characteristics were determined using an H-type electrochemical cell.

2. Experimental

2.1. Electrolytes

Electrolytic solutions were prepared by dissolving $Mn(acac)_3$ (90%, Strem, U.S.) and $TEABF_4$ (99%, Fluka, U.S.) in anhydrous CH_3CN (99.8%, Aldrich, U.S.). Concentrations for $Mn(acac)_3$ and $TEABF_4$ were 0.05 M and 0.5 M, respectively.

2.2. Cyclic voltammetry experiments

Cyclic voltammetry was performed using an Autolab PGSTAT302N Potentiostat/Galvanostat (Ecochemie, Netherlands).

* Corresponding author at: Department of Chemical Engineering, University of Michigan, 2300 Hayward Street, Ann Arbor, MI 48109-2136, USA.
Tel.: +1 734 936 2019; fax: +1 734 763 0459.
E-mail address: ltt@umich.edu (L.T. Thompson).

0378-7753/$ – see front matter © 2011 Elsevier B.V. All rights reserved.
doi:10.1016/j.jpowsour.2011.02.020

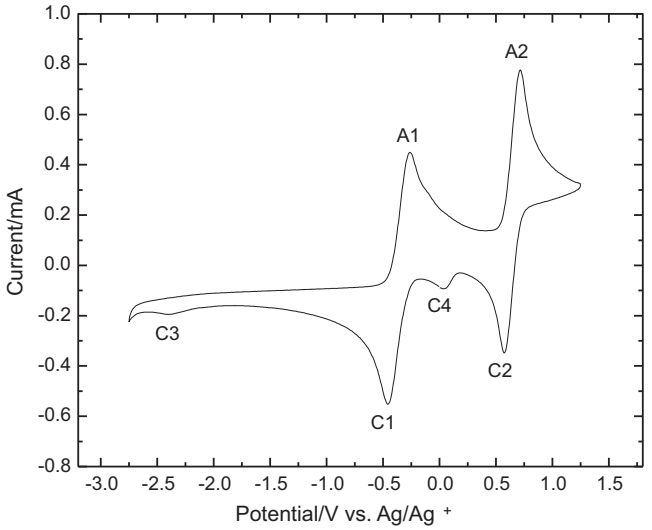

Fig. 1. Cyclic voltammograms measured at a glassy carbon electrode in 0.05 M $Mn(acac)_3$ and 0.5 M $TEABF_4$ in CH_3CN; scan rate 100 mV s^{-1}; room temperature.

A 3 mm diameter glassy carbon electrode (BASi, U.S.) was used as the working electrode. The working electrode was polished with 1200 grit silicon carbide polishing paper, ultrasonically cleaned and rinsed thoroughly with distilled water. Potentials during CV were measured relative to a 0.01 M Ag/Ag^+ and 0.1 M tetraethylammonium perchlorate ($TEAClO_4$) reference electrode, which was connected to the working-electrode chamber via a Luggin capillary. A large-area (~9 cm^2) graphite plate (Graphitestore, U.S.) was used as the counter electrode. Solutions were purged with research-grade nitrogen prior to the experiments.

2.3. Charge–discharge experiments

An H-type glass cell was used for the charge–discharge experiments [7,9]. Each compartment contained 10 mL of electrolytic solution that was continuously agitated using a Teflon magnetic stir-bar. The electrolytes were separated by a Neosepta AHA anion-exchange membrane (Astom, Japan). Prior to each experiment, the membranes were pre-conditioned by soaking in a solution containing 0.5 M $TEABF_4$ in CH_3CN for more than 22 h. Two graphite electrodes were employed in the charge–discharge experiments, with immersed surface areas of 7 cm^2. Galvanostatic conditions were used, with charge and discharge currents of 1.0 mA and 0.4 mA, respectively. The cells were charged up to a potential cutoff of 1.2 V and discharged down to 0.04 V. All charge–discharge experiments were performed in an argon-filled glove box.

3. Results and discussion

3.1. Voltammetric behavior of $Mn(acac)_3$ in acetonitrile

Fig. 1 shows the CV for a solution containing 0.05 M $Mn(acac)_3$ and 0.5 M $TEABF_4$ in CH_3CN cycled at 100 mV s^{-1}. The maximum solubility of $Mn(acac)_3$ in CH_3CN was measured to be ~0.6 M at room temperature. The concentration for these experiments was kept low to allow for investigation of the electrochemistry under conditions where the thermodynamics and transport are expected to be relatively ideal.

Two redox couples were observed within the solvent stability window, at −0.4 and 0.7 V vs. Ag/Ag^+. The electrochemistry of manganese acetylacetonate has been evaluated in a range of electrolytes and with different electrode materials [12–15]. Gritzner et al. defined the $Mn(acac)_3$ redox potentials at Pt and Hg using solvents including CH_3CN, with tetrabutylammonium perchlorate supporting electrolyte [13]. Peak potentials and kinetics were observed to be highly dependent on solvent, supporting electrolyte and electrode material. They reported redox couples at 0.64 and 1.70 V vs. a bis(biphenyl)chromium tetraphenylborate/bis(biphenyl)chromium reference electrode. Although differences in the reference electrodes used makes it difficult to compare the absolute values of these redox potentials to those reported here, the voltage differences between the redox couples (~1.1 V) are consistent. Given the similarities, we have assigned the redox couples observed here to the reactions:

$$\text{A1/C1}: \ Mn^{III}(acac)_3 + e^- \leftrightarrow [Mn^{II}(acac)_3]^- \qquad E = -0.4 \text{ V vs. } Ag/Ag^+ \tag{1}$$

$$\text{A2/C2}: \ Mn^{III}(acac)_3 \leftrightarrow [Mn^{IV}(acac)_3]^+ + e^- \qquad E = 0.7 \text{ V vs. } Ag/Ag^+ \tag{2}$$

Features associated with half-reactions (1) and (2) are labeled in Fig. 1. Formal potentials for each reaction were estimated by taking the average of the anodic and cathodic peak potentials. The formal potentials indicated that an RFB system based on the one-electron disproportionation of $Mn(acac)_3$ would yield a 1.1 V cell potential. This is comparable to the aqueous vanadium RFB system (1.26 V under standard conditions [16]) but much smaller than the 2.2 and 3.4 V reported for the non-aqueous $V(acac)_3$ [9] and $Cr(acac)_3$ [10] systems, respectively.

Two additional reduction peaks, labeled C3 and C4, can be seen in Fig. 1. In CH_3CN solvent, Gritzner et al. reported a peak corresponding to a second reduction of $Mn(acac)_3$ at −1.49 V vs. bis(biphenyl)chromium tetraphenylborate/bis(biphenyl)chromium [13]. Again, due to differences in reference electrodes, it is difficult to compare absolute values for potential, but because Gritzner et al. reported the first reduction of $Mn(acac)_3$ at 0.64 V, we would expect this second reduction at a potential ~2.1 V negative of the first reduction. From Fig. 1 it can be seen that the formal potential of the peak labeled C3 is −2.4 V vs. Ag/Ag^+, or ~2 V more negative than the A1/C1 redox couple. In the report by Gritzner et al., this second reduction peak was not assigned to a particular Mn oxidation state. From reports of the electrochemistry of other Mn complexes in organic solvents [17,18], in which peaks corresponding to the second reduction of Mn observed at very negative potentials were attributed to the reduction of Mn^{II} to Mn^0, it seems likely that the reduction peak observed in this work similarly corresponds to the two-electron reduction to metallic Mn. This reduction peak, C3, has consequently been attributed to the reaction:

$$\text{C3}: \ [Mn^{II}(acac)_3]^- + 2e^- \leftrightarrow [Mn^0(acac)_3]^{3-} \qquad E = -2.4 \text{ V vs. } Ag/Ag^+ \tag{3}$$

The lack of an observable corresponding oxidation peak suggests that reaction 3 is coulombically irreversible and would not be useful for a rechargeable RFB.

The peak in Fig. 1 labeled C4 at 0 V vs. Ag/Ag^+ was not observed in the $Mn(acac)_3$ voltammetry reported by Gritzner et al. [13]. Although the origin of peak C4 has not been determined unambiguously, one possibility is that it stems from the presence of H_2O in the system. The $Mn(acac)_3$ complex used in this research contained ~10% H_2O. The peak does not appear to owe to ligand shedding because there were no peaks observed in the cyclic voltammograms near 0 V vs. Ag/Ag^+ when acetylacetone was added to a 0.5 M

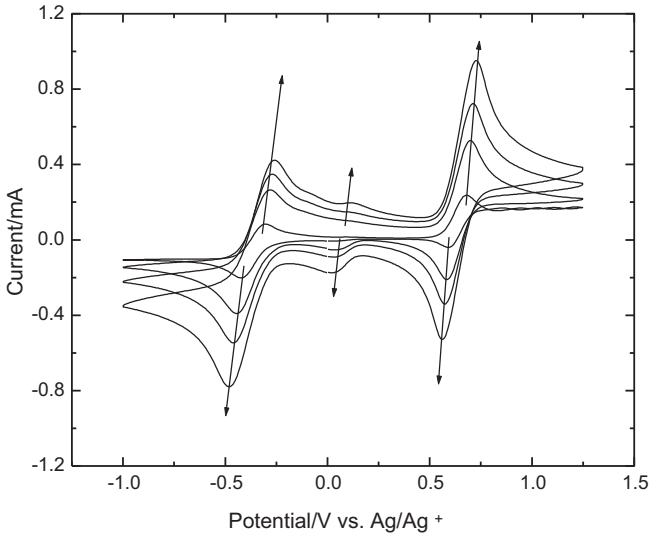

Fig. 2. Cyclic voltammograms measured at a glassy carbon electrode in 0.05 M $Mn(acac)_3$ and 0.5 M $TEABF_4$ in CH_3CN at scan rates of 10, 50, 100, and 200 mV s^{-1}, arrows show direction of increasing scan rate; room temperature.

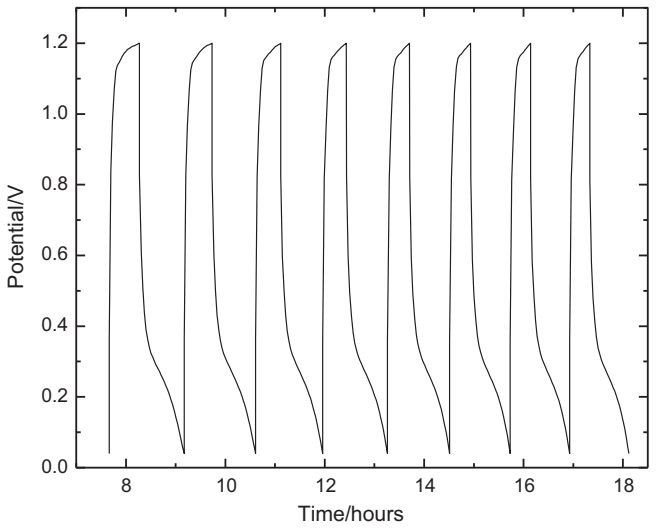

Fig. 3. Charge–discharge curves for 0.05 M $Mn(acac)_3$ and 0.5 M $TEABF_4$ in CH_3CN; charge current 1 mA with 1.2 V cutoff and discharge current 0.4 mA with 0.04 V cutoff; room temperature.

$TEABF_4$ in CH_3CN solution. Further investigation is needed to elucidate the origin of this peak, especially as it may affect the efficiency of the RFB cell during cycling.

3.2. Kinetics of electrode reactions

Fig. 2 shows a series of cyclic voltammograms at varying scan rates for 0.05 M $Mn(acac)_3$ and 0.5 M $TEABF_4$ in CH_3CN. For the Mn^{II}/Mn^{III} redox couple, the peak separation, ΔE_p, increased from 120 to 290 mV as the scan rate increased from 10 to 500 mV s^{-1}. Similarly, for the Mn^{III}/Mn^{IV} redox couple, ΔE_p increased from 90 to 210 mV with increasing scan rate. For both redox couples, ratios of the anodic to cathodic peak currents were near unity. These observations indicate quasi-reversible electrode kinetics. An oxidation peak associated with anomalous peak C4 can also be observed in Fig. 2. The peak heights for this redox couple increased with increasing scan rate.

To determine the diffusion coefficient for $Mn(acac)_3$ in the electrolytic solution, changes in peak height were measured as the scan rates were varied from 10 to 500 mV s^{-1}. Because the redox couples appear to show quasi-reversible kinetics, relationships for reversible and irreversible reactions were investigated. For a reversible redox couple, the peak current i_p is given by the Randles–Sevcik equation [19]:

$$i_p = 2.69 \times 10^5 n^{3/2} A C D_o^{1/2} v^{1/2} \quad (4)$$

where n is the number of electrons transferred in the electrode reaction ($n = 1$), A the electrode area (0.07 cm^2), C the bulk active-species concentration, D_o the active-species diffusion coefficient, and v the scan rate. A plot of i_p vs. $v^{1/2}$ yields a straight line with a slope proportional to D_o. Based on the cathodic peak current for the Mn^{II}/Mn^{III} redox couple, the diffusion coefficient for $Mn(acac)_3$ in a supporting electrolyte of 0.5 M $TEABF_4$ in CH_3CN was estimated to be 3.0×10^{-6} cm^2 s^{-1}. For an irreversible redox couple, the peak current is governed by [19]:

$$i_p = 2.99 \times 10^5 n^{3/2} \alpha^{1/2} A C D_o^{1/2} v^{1/2} \quad (5)$$

Using this relationship, the $Mn(acac)_3$ diffusion coefficient was estimated to be 4.8×10^{-6} $cm^2 s^{-1}$. Given these results, we expect the value for the diffusion coefficient of the neutral complex to be in the range of $3–5 \times 10^{-6}$ cm^2 s^{-1}. This is comparable to that for $V(acac)_3$ in the same supporting electrolyte and solvent [9] and approximately an order of magnitude higher than that reported for $Cr(acac)_3$ [10].

3.3. Charge–discharge performance

Charge–discharge characteristics for a cell containing 0.05 M $Mn(acac)_3$ and 0.5 M $TEABF_4$ in CH_3CN were evaluated. Galvanostatic conditions were used with potential cutoffs for both charge and discharge. The charge cutoff was 1.2 V, slightly higher than the 1.1 V cell potential observed in the voltammetry for the one-electron disproportionation of $Mn(acac)_3$. This potential should prevent the irreversible reduction of Mn^{II} to Mn^0 which was observed in the voltammetry at ~−2.4 V and which has a cell potential in combination with the $Mn^{III/IV}$ redox couple of ~3.1 V. The discharge cutoff was set at 0.04 V to allow the system to fully discharge without introducing side reactions. Fig. 3 illustrates cycles 3–10. One discharge plateau is observed at ~0.3 V for all ten cycles. This likely corresponds to the one-electron disproportionation of the $Mn(acac)_3$ species which has a cell potential of 1.1 V. The charge and discharge voltages were respectively higher and lower than the cell voltages determined by CV. In the H-cell configuration, the electrodes were separated by a significant distance (~10 cm). Given this, the 0.5 M concentration of the support, and the presence of the anion-exchange membrane separator, ohmic overpotentials were probably significant.

Coulombic efficiencies increased steadily from ~74% for cycle 3 to ~97% for cycle 10. This increase with cycle number owes to an unknown side reaction, with one possibility being corrosion of the electrode material. Energy efficiencies were reasonably constant at ~21% over the cycles suggesting that the use of the voltage cutoffs prevented the irreversible reduction of Mn^{III} to Mn^0.

4. Conclusions

A manganese acetylacetonate active species was evaluated for application in non-aqueous RFBs, using a tetraethylammonium tetrafluoroborate/acetonitrile supporting electrolyte. Results from cyclic voltammetry indicated that the $Mn(acac)_3$ complex can be oxidized to $[Mn(acac)_3]^+$ and reduced to $[Mn(acac)_3]^-$ at a glassy carbon electrode. The anodic and cathodic half-cell reactions appeared to be electrochemically quasi-reversible and the cell potential was 1.1 V. This potential is comparable to aqueous

vanadium RFB systems, but much smaller than cell potentials reported for other non-aqueous RFB chemistries. A second, irreversible, reduction to $[Mn(acac)_3]^{3-}$ was observed at very negative potential.

The charge–discharge characteristics for an electrolyte containing 0.05 M $Mn(acac)_3$ and 0.5 M $TEABF_4$ in CH_3CN were evaluated in an H-type cell using a membrane separator. One discharge plateau was observed at ~0.3 V which is thought to correspond to the one-electron disproportionation of the $Mn(acac)_3$ complex. Coulombic efficiencies were observed to increase with cycle number suggesting a side reaction. Energy efficiencies were reasonably constant at ~21%.

Acknowledgements

The authors acknowledge financial support from the Advanced Energy for Transportation Technology Program and the Hydrogen Energy Technology Laboratory.

References

[1] H.S. Lim, A.M. Lackner, R.C. Knechtli, J. Electrochem. Soc. 124 (1977) 1154–1157.
[2] N.H. Hagedorn, L.H. Thaller, Power Sources 8 (1981) 227–243.
[3] A. Price, S. Bartley, S. Male, G. Cooley, Power Eng. J. 13 (1999) 122.
[4] E. Sum, M. Rychcik, M. Skyllas-Kazacos, J. Power Sources 16 (1985) 85–95.
[5] E. Sum, M. Skyllas-Kazacos, J. Power Sources 15 (1985) 179–190.
[6] Y. Matsuda, K. Tanaka, M. Okada, Y. Takasu, M. Morita, T. Matsumura-Inoue, J. Appl. Electrochem. 18 (1988) 909–914.
[7] M.H. Chakrabarti, R.A.W. Dryfe, E.P.L. Roberts, Electrochim. Acta 52 (2007) 2189–2195.
[8] T. Yamamura, Y. Shiokawa, H. Yamana, H. Moriyama, Electrochim. Acta 48 (2002) 43–50.
[9] Q. Liu, A.E.S. Sleightholme, A.A. Shinkle, Y. Li, L.T. Thompson, Electrochem. Commun. 11 (2009) 2312–2315.
[10] Q. Liu, A. Shinkle, Y. Li, C. Monroe, L. Thompson, A.E.S. Sleightholme, Electrochem. Commun. 12 (2010) 1634–1637.
[11] F.-Q. Xue, Y.-L. Wang, W.-H. Wang, X.-D. Wang, Electrochim. Acta 53 (2008) 6636–6642.
[12] G. Gritzner, H. Murauer, V. Gutmann, J. Electroanal. Chem. Interfacial Electrochem. 101 (1979) 177–183.
[13] G. Gritzner, H. Murauer, V. Gutmann, J. Electroanal. Chem. Interfacial Electrochem. 101 (1979) 185–200.
[14] O. Sock, P. Lemoine, M. Gross, Electrochim. Acta 26 (1981) 99–109.
[15] K. Yamaguchi, D.T. Sawyer, Inorg. Chem. 24 (1985) 971–976.
[16] C. Ponce de Leon, A. Frias-Ferrer, J. Gonzalez-Garcia, D.A. Szanto, F.C. Walsh, J. Power Sources 160 (2006) 716–732.
[17] M.E. Bodini, V.M. Arancibia, Polyhedron 11 (1992) 2195–2202.
[18] F.C. Frederick, K.E. Johnson, J. Electrochem. Soc. 128 (1981) 2070–2073.
[19] A.J. Bard, L.R. Faulkner, Electrochemical Methods—Fundamentals and Applications, Wiley, second ed., 2001.